

# Implementation of Virtual Instrumentation for Testing of Induction Motors

Gheorghe-Eugen Subtirelu

University of Craiova/Faculty of Electrical Engineering, Craiova, Romania, esubtirelu@em.ucv.ro

**Abstract** - This paper presents an implementation of an advanced system that uses virtual instrumentation as the main component in the process of measurement and testing of three phase asynchronous motors. This approach permits the replacement of the old analog measurement techniques – which are still in use in the industry applications at some electrical motor testing benches, with the new advanced measurement system bench. This system bench is capable of data acquisition, storage on different media, visualization of relevant graphs, printing or distribution of technical reports or analysis on-line or off-line in an automated manner. The general architecture of the proposed system is focused on the hardware components (transducers, conditioning, data acquisition, calculator) and software components (driver for the acquisition and manipulation-calculation of data, graphical presentation, other auxiliary programs and the ones to bring all the components together, virtual instruments). The proposed system allows the application of methods for determining losses and efficiency from tests. Some of the most important requirements of the international standards for induction motors testing are used: general technical verification, determination of the windings resistance in DC, no-load testing and running characteristics testing. This system would be very useful in industry applications in the domains of electrical machines for testing workbenches and design laboratories.

**Cuvinte cheie:** *instrumentație computerizată, achiziție de date, testarea motoarelor de inducție, interpolare cu funcții polinomiale și spline, extrapolare.*

**Keywords:** *computerized instrumentation, data acquisition, induction motors testing, interpolation with polynomial and spline functions, extrapolation.*

## I. INTRODUCTION

The increase in the number of electric drives in all areas of life (industry, agriculture, transport, medicine, etc.) implies an increase in the number and technical performance of electric machines. Thus, in many applications three-phase induction motors are widely used due to their rugged, robust, low priced and easy to maintain features.

Testing of electric machines is an important stage, both in the research and development stage and before they are placed on the market. The main objective of this paper is to solve a practical current problem, by taking advantage of the new technology. The new technology is based on graphical software LabVIEW and it is used for interpreting digital measurements and the automation of the technical data for testing of three-phase induction machine. This new trend in testing electrical machines can deliver the technical reports automatically; also, it always saves resources and costs.

General aspects and theory concepts for electrical machines testing, virtual instrumentation and data acquisition (DAQ) are used for design of the proposed system [1], [2], [8].

The most important requirements of the international standards for testing three-phase induction motors are used for: general technical verification, determination of the windings resistance in DC, no-load testing and running characteristics testing [12]-[15].

These will constitute the theoretical basis for the document elaboration and will be briefly presented in the next chapter.

The construction of the virtual instruments (VIs) will be presented in detail, to offer a better view of the capability of this new concept.

The system can be updated in the future with modular data acquisition hardware (i.e. for torque, temperature, vibration or noise-level measurements) and other virtual instruments to complete the induction machine test list: locked rotor (short-circuit) testing, temperature-rise testing, overvoltage between turns testing, noise-level measurement and so on.

With this system can be created flexible test applications that can control multiple instruments (transducers) and design user interfaces using LabVIEW to optimize induction machine testing and operational cost.

The implementation of the virtual instrumentation for a few tests of induction motors was presented in previous papers [3], [4], [5]. Here, I updated the measurement system with another virtual instrument that allows the determination of functional characteristics of induction motor in load test.

## II. THEORETICAL ASPECTS

The theory of the induction motors are very well know and will not insist on it. I will present a few formulas used to design virtual instruments which compose the system. The program of testing is established in accordance with applied standards based on initial data of the motor (type, parameters rating) and type of testing. Four types of tests are selected and briefly described [15].

### A. General technical verification

This is the first element of any machine test program. The three-phase squirrel-cage motors have a few general technical requirements to be checked [12]-[15].

### B. DC stator winding measurement on cold state

Measuring winding resistance is not a difficult problem because we have access to the terminals; the indirect method is used.

If the windings are wye connection, then two windings are connected in series between two terminals. If the windings are delta connection, then two branches are connected in parallel between two terminals: a branch consists of the resistance of one phase and the other branch consists of the other two phases in series.

It is known that the resistance varies with temperature. Thus, knowing the value of the winding resistance at a certain ambient temperature ( $R_l$  at  $T_{amb}$ ), we calculate the value of the winding resistance at another temperature ( $R_l$  at  $T_l$ , where  $T_l$  is  $75^\circ\text{C}$  or  $115^\circ\text{C}$ , depending on the class of stator insulation) using the formula:

$$R_{l_{Tl}} = R_{l_{Tamb}}[1 + \alpha(T_l - T_{amb})] \quad (1)$$

where  $\alpha$  is the temperature coefficient of winding resistance.

### C. No-load test

When an induction motor runs at no-load, the slip is very small.

The values of no-load power  $P_0$ , current  $I_0$ , power factor  $PF_0$ , mechanical and ventilation losses  $P_{mv}$ , iron losses  $P_{iron}$  and Joule stator losses  $P_{Joule0}$  can be found by the following test. Their values can be determined by measuring the voltages, currents and power at no-load as follows:

-the motor under test connects to the power grid and running no-load at nominal voltage  $U_N$ ;

-the voltage is increased to about  $1.3 U_N$ ; then the voltage is decreasing from approx.  $130\% U_N$  down to zero, using the voltage regulator;

-complete a table for minimum eleven decreasing values of voltage; the voltage is reduced to the value at which the current (and slip) starts to rise;

-we will use the eleven measured points to plot the graphs: current  $I_0 = f(U_0)$  and total three-phase active power  $P_0 = f(U_0)$ . From these eleven original points on the graphs, using interpolation are obtained (for the nominal voltage  $U_N$ ) the values of current  $I_0$  and no-load power  $P_0$  (Fig.1);

-the power factor  $PF_0$  is obtained with the next formula:

$$PF_0 = P_0 / \sqrt{3} U_0 I_0 \quad (2)$$

-after the test will measure stator winding resistance  $R_{l0}$  and determine Joule stator losses  $P_{Joule0}$ :

$$P_{Joule0} = R_{l0} I_0^2 \quad (3)$$

for the delta windings connection or:

$$P_{Joule0} = 3R_{l0} I_0^2 \quad (4)$$

for the wye windings connection of stator.

Now the motor's losses are divided into three main components: the Joule losses in the winding  $P_{Joule0}$ ; the mechanical and ventilation losses  $P_{mv}$ ; the iron losses  $P_{iron}$ .

The mechanical/ventilation and iron losses results from the formula:

$$P_{mv} + P_{iron} = P_0 - P_{Joule0} \quad (5)$$

Fig.1 shows the graph of the loss separation after the no-load testing. The loss curve (5) is plotted against the square of voltage; in the point of abscissa 0, the voltage is 0 and the iron losses are zero [15].

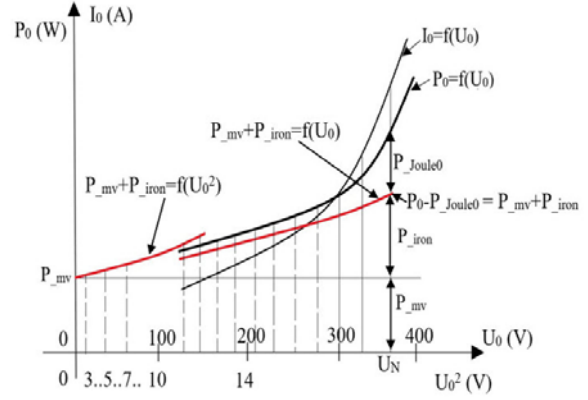


Fig. 1. The separation of loss in the no-load testing.

The mechanical and ventilation losses does not depend on voltage  $U_0$ ; they are determined by plotting the graph  $P_0$  and  $P_0 - P_{Joule0}$  with the abscissa  $U_0$ ; the  $P_{mv}$  curve is extrapolated to the Oy axis where  $U_0$  is zero (see also the above relation and Fig. 1) [12]-[15].

### D. Running characteristics in load test

The functional (running) characteristics can be determined according to the output power  $P_2$  of the motor; they are determined by direct loading at rated voltage ( $U_{lN}$ ) and frequency ( $f_N$ ).

The following dependencies will be drawn graphically:  $I_l = f(P_2)$ ,  $P_l = f(P_2)$ ,  $PF = \cos\varphi = f(P_2)$ ,  $s = f(P_2)$  and  $\eta = f(P_2)$ .

In order to raise all these characteristics are measured following sizes: line voltage  $U_l$ , the power supply frequency, the line currents  $I_l$ , power absorbed  $P_l$  and speed  $n_2$ .

Complete a table for five useful power values ranging between  $(1.25 \dots 0.25) P_{2N}$ . The formulas used are the following:

-the power factor  $PF$ :

$$PF = P_l / \sqrt{3} U_l I_l \quad (6)$$

-after the heating test will measure stator winding resistance  $R_l$  and determine Joule stator losses  $P_{Joule1}$  with relations (3) or (4), depending on connection type;

-the iron losses  $P_{iron}$  were determined at no-load test;

-the electromagnetic power transmitted by the stator:

$$P_{12} = P_l - (P_{Joule1} + P_{iron}) \quad (7)$$

-Joule rotor losses  $P_{Joule2}$  result:

$$P_{Joule2} = s \cdot P_{12} / 100 \quad (8)$$

-the mechanical and ventilation losses  $P_{mv}$  were determined at no-load test;

-additional (stray-load) losses are:

$$P_{add} = 0,005 \cdot P_l \quad (9)$$

-the output (useful) power  $P_2$ :

$$P_2 = P_l - (P_{Joule2} + P_{mv} + P_{add}) \quad (10)$$

-the efficiency of motor:

$$\eta = 100 \cdot P_2 / P_l \quad (11)$$

### III. HARDWARE OF SYSTEM

Fig. 2 shows the block diagram of the system used to test the induction motors; both the measurement system and the power supply side are presented in the block diagram.

The most important elements of the measurement system are: NI-DAQ module with conditioning / adapting elements and LEM current (3) and voltage transducers (3).

A speed transducer is required for the determination of functional characteristics in load test (running characteristics testing).

The tested induction motor (UUT) is powered from the grid via a main switch (K) and a voltage regulator (VR).

NI-USB DAQ module type 6210 has the following main features: 16 analog inputs (16 single ended, 8 differential), 16-bit resolution, 250 kS/s sampling frequency, multifunction digital I/O.

Fig. 3 shows the module block of transducers. I designed this module having in mind other future complex applications (e.g., to study the dynamic and transient regime occurring in starting, braking and speed control of electric machines); the number of analog inputs is greater than the ones required and we also added a number of 4 digital inputs / outputs for quick command of contacts.

I used 6 non-inductive transducers LEM, type PBT LV 25-P (500V) for 6 voltage measurements and 3 transducers type PBT LA 100-P (100A) for 3 current measurements, all with galvanic isolation.

The signal produced by adapting and conditioning circuitry associated with LEM transducers is in the form of voltage signal sources which are applied to six analog inputs (AI) of DAQ module (AI0 to AI5).

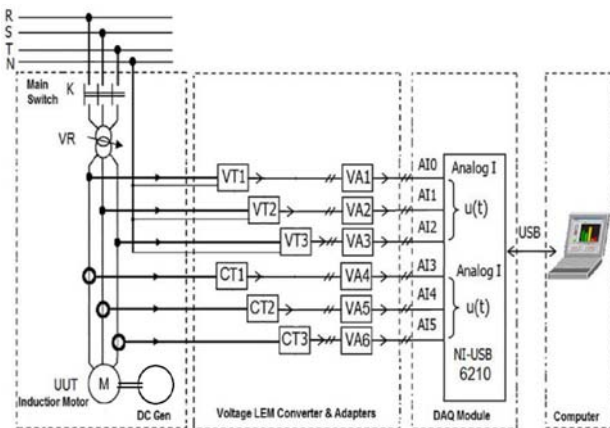


Fig. 2. Hardware components of the advanced test system.

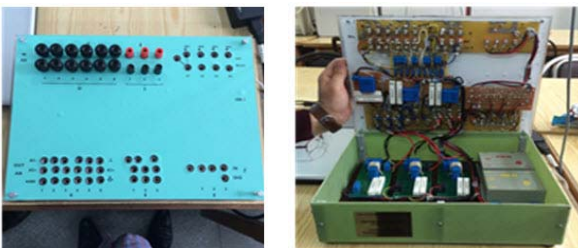


Fig. 3. The module block of transducers.

### IV. VIRTUAL INSTRUMENTS OF SYSTEM

Here I will build seven virtual instruments which are working with proposed system: *Program Start Menu.vi*; *Initial Test Data.vi*; *Testing Program.vi*; *General Technical Verification.vi*; *DC Stator Winding Resistance on Cold State.vi*; *No-Load Test.vi* and *Running-Characteristics Test.vi*.

The first three are general for the system and the rest perform the motor tests.

#### A. General virtual instruments

Fig. 4 presents the user interface of the program. Select one of the options in the menu by double clicking to each and will begin to work with the virtual instrument. Only one VI runs at a time. Use *Exit* button to stop running the VI.

The block diagram is given in Fig. 5. The three virtual instruments are used as sub diagrams in a *Case structure* that executes only one of them.

Fig. 6 presents the frontal panel for *Initial Test Data.vi*; with this interface the operator can introduce data about: the identification of testing laboratory, client and order; the motor under test; experimental, type or series testing; technical documents.

Fig.7 shows the frontal panel of virtual instrument which chooses the testing program for motor under test (three in this example).

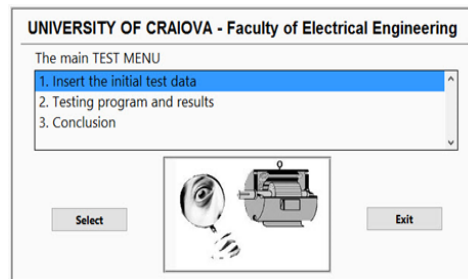


Fig. 4. The front panel of *Program Start Menu.vi*.

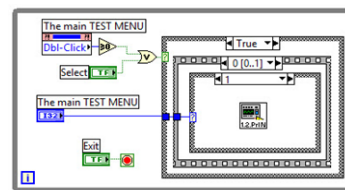


Fig. 5. The block diagram of *Program Start Menu.vi*.

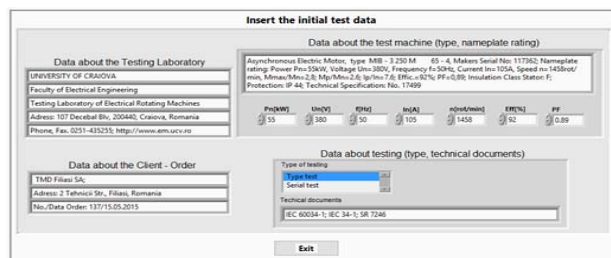


Fig. 6. The front panel of *Initial Test Data.vi*.

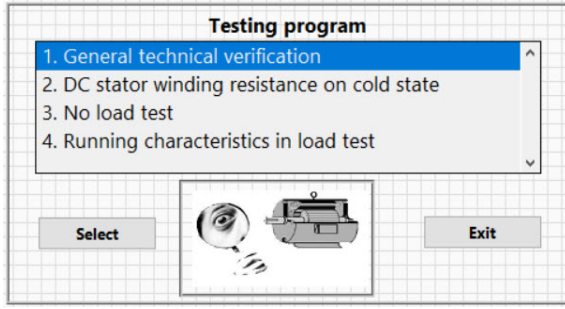


Fig. 7. The front panel of *Testing Program*.vi.

### B. Virtual instrument for general technical verification

Fig. 8 presents the user interface to insert the information about evaluation of general technical motor's requirements: checked if the general assembly is in accordance with the drawing; screws and nuts are tight; rotor rotates freely, without friction; nameplate is properly inscribed.

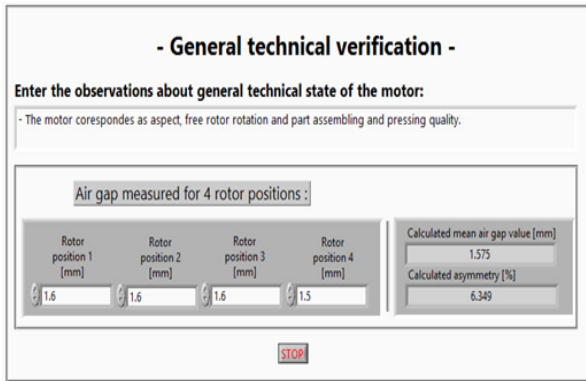


Fig. 8. The front panel of *General Technical Verification*.vi.

The calculating (Asym) asymmetry of the air gap is done with the formula:

$$Asym = (Max - Min)/Mean \cdot 100 \quad (12)$$

where: *Asym* is the asymmetry of air gap and *Max*, *Min*, *Mean* are the maximum, minimum and mean values of air gap for four positions of the rotor.

### C. Virtual instrument for DC stator winding measurement on cold state

Fig. 9 presents the user interface to determine the DC Stator Winding Resistance on Cold State. The virtual instrument can work independently (Simulation mode or On-Line Acquisition mode) or integrated as part of a measurement system.

With a List box control, one of the variants of the stator winding connection is chosen. The simplified layout schemas for each case are on the right side of the List box control.

The measured DC voltage and current through each test are listed in a table. The resistance value between two measuring points is calculated as the ratio between voltage and current. Write each line in the table using the 'VALIDATION of Point' button. Pressing the 'RESET Table' button the operator can delete the data entered in the table.

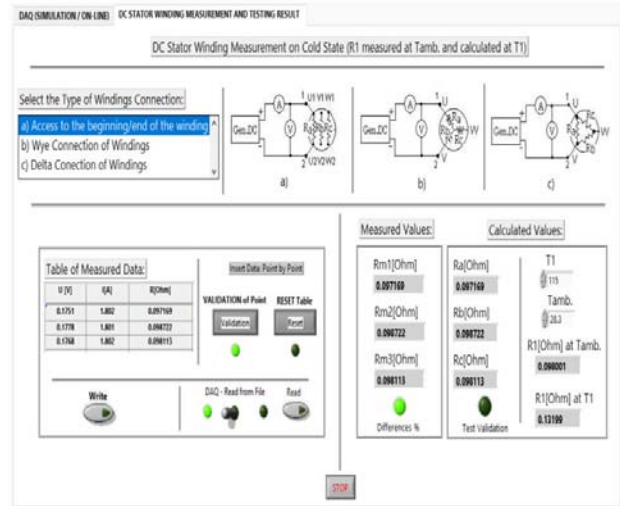


Fig. 9. The front panel of *DC Stator Winding Resistance on Cold State*.vi.

The 'Differences %' LED illuminates if there are differences between the measured values (*Rm1*, *Rm2*, *Rm3*) which are greater than 2% for the wye connection and 1.5% for delta connection of windings [15]. The 'Test Validation' LED illuminates when the three (*Rm1*, *Rm2*, *Rm3*) values are available to make the next calculations.

The resistance values of the three phase windings (*Ra*, *Rb*, *Rc*) are calculated.

The resistance value of a stator phase (*R<sub>i</sub>*) at ambient temperature (*Tamb*) and the value corrected at the temperature (*T<sub>i</sub>*) required by the standards according to the motor's insulation class are also calculated.

The values of (*Tamb*) and (*T<sub>i</sub>*) are entered using numeric controls.

### D. Virtual instrument for no-load test

The virtual instrument for no-load test is composed of three pages: the first page of control is used to determine how to obtain the input data of the instrument (we can choose between a simulation or an acquisition on-line).

The specific parameters for data acquisition can be found in this page: sample mode, number of samples, sample rate.

The second page of control is for presentation of six sets of measured or simulated data (three voltages and three currents) and other calculated quantities required for the test (*U<sub>0</sub>*, *I<sub>0</sub>*, *P<sub>0</sub>*).

Fig. 10 shows the third page of virtual instrument: data processing and presentation of the testing results.

The voltage, current and power values are displayed in the numeric indicators on the left corner. The values of winding resistance *R<sub>10</sub>* after no-load test is input by numeric control and is used for calculating winding losses.

The mechanical/ventilation and iron losses are plotted against the square of voltage; the *P<sub>mv</sub>* value is determined by extrapolation in the point of abscissa 0 (see also Fig. 1). The resulting values are displayed in numeric indicators.

The curves *I<sub>0</sub> = f(U<sub>0</sub>)* and *P<sub>0</sub> = f(U<sub>0</sub>)* can be drawn in two ways: by fitting curves (approximation between points) – plot 1, red color and even through the given points – plot 0, black color.

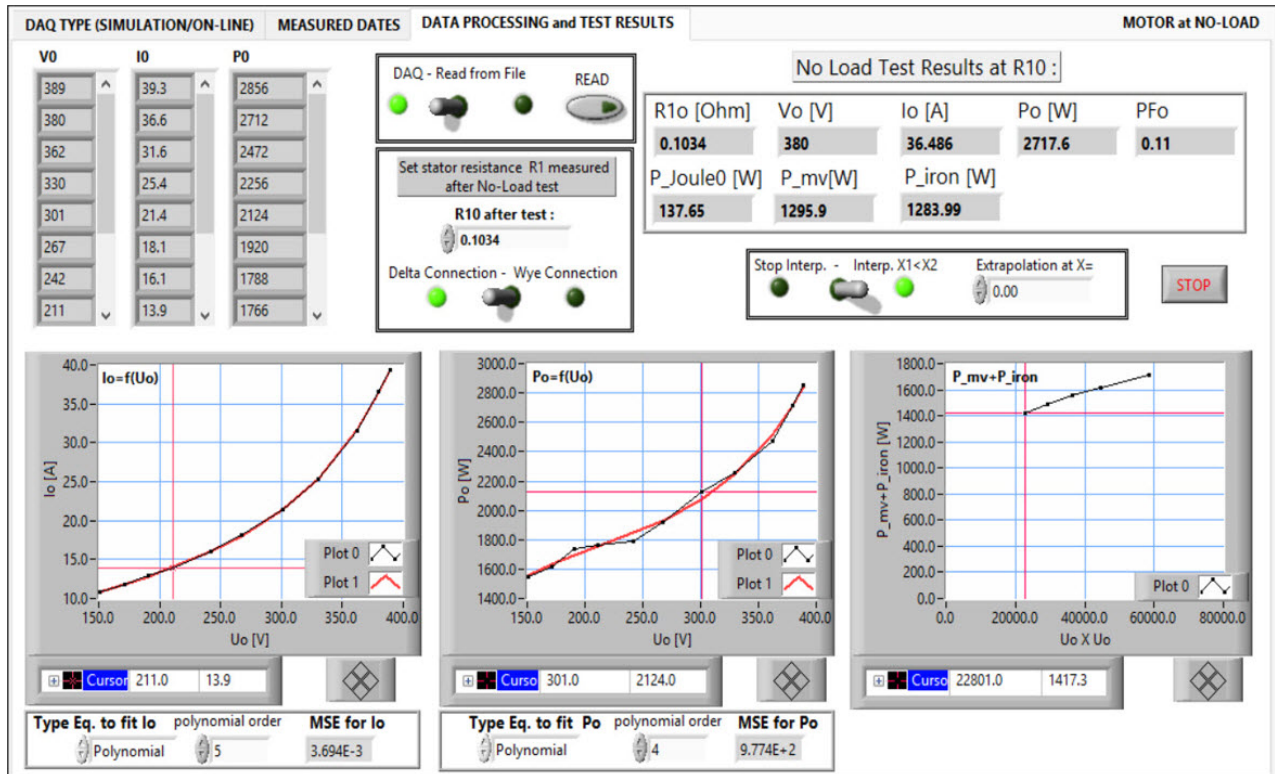


Fig. 10. The front panel of *No - Load Test.vi*.

To draw curves by fitting I used linear functions provided by LabVIEW. The best results were obtained using polynomial functions: for the curve  $I_0 = f(U_0)$ , the best estimate is given by a polynomial function of order 5 (Mean of Square Error is  $3.694E-3$ ); for the curve  $P_0 = f(U_0)$ , the polynomial function of order 4 offers the best estimate because Mean of Square Error is  $9.774E+2$ ).

In order to choose the correct function, it is necessary to observe that these curves have a regular appearance, smooth, seamless, oscillations or loops between set points and determine the media square error of each drawing point.

#### E. Virtual instrument for determination of functional characteristics in load test

Figure 11 shows the second page of virtual instrument for determination of functional characteristics in load test, respectively the measured data.

In the table located at the top of the front panel are entered, by validation using the VALIDATION POINT button, the sets of 7 acquired signals: 3-line voltages, 3-line currents and motor speed. To delete all data in the table, press the RESET Table button.

The data can also be entered later, an option made and signaled by switching the Data Table toggle switch to the left position.

To save the data acquired and tabulated set WRITE button; so, the data will be saved in a user-selected directory in the spreadsheet string format (date and time of testing is included).

Also, same controls and indicators are provided for the rated motor parameters (from *Initial Test Data.vi*) and to the values obtained from previous tests (e.g., *No-Load Test.vi*).

With the STOP button, it turns off the virtual instrument if it works independently or goes to another VI if it works in an integrated system.

Figure 12 shows the third page of virtual instrument; here, the data are processed and the test results are presented.

There are several numeric indicators in the top left of the front panel; here are displayed the values acquired for voltage ( $V$ ), current ( $I$ ), power absorbed ( $P$ ) and motor speed ( $n_2$ ) in 5 measuring points; also are displayed parameters whose value was obtained from the previous test (e.g., the iron losses  $P_{iron}$  and the mechanical/ventilation losses  $P_{mv}$  determined from *No-Load Test*).

Using these data are calculated with formulas (6) to (11) the other required parameters ( $PF$ ,  $P_{Joule1}$ ,  $P_{Joule2}$ ,  $P_{12}$ ,  $P_{add}$ ,  $P_2$ ).

A numeric control allows insertion the synchronous speed  $n_1$  [rpm] to be used in calculating the motor slip  $s$  with the following formula:

$$s = 100 \cdot (n_1 - n_2) / n_1 \quad (13)$$

The value of corrected  $R_1$  resistance of stator windings (e.g. for  $75^\circ\text{C}$  or  $115^\circ\text{C}$ ) is introduced to be used for calculating losses in stator windings  $P_{Joule1}$ . The efficiency of induction motor is determined by the separate loss method.

The curves  $P_1 = f(P_2)$ ,  $I_1 = f(P_2)$ ,  $s = f(P_2)$ ,  $\eta = f(P_2)$  and  $PF = \cos\varphi = f(P_2)$  are plotted by fitting curves (by polynomial functions) and even through the given points.

On the graphs plotted (at the nominal output power  $P_{2N}$ ) the values of the following parameters are determined:  $P_1$ ,  $I_1$ ,  $s$ ,  $\eta$  and  $PF$ . They are determined by spline interpolation function. These parameters characterize the motor running in the load.

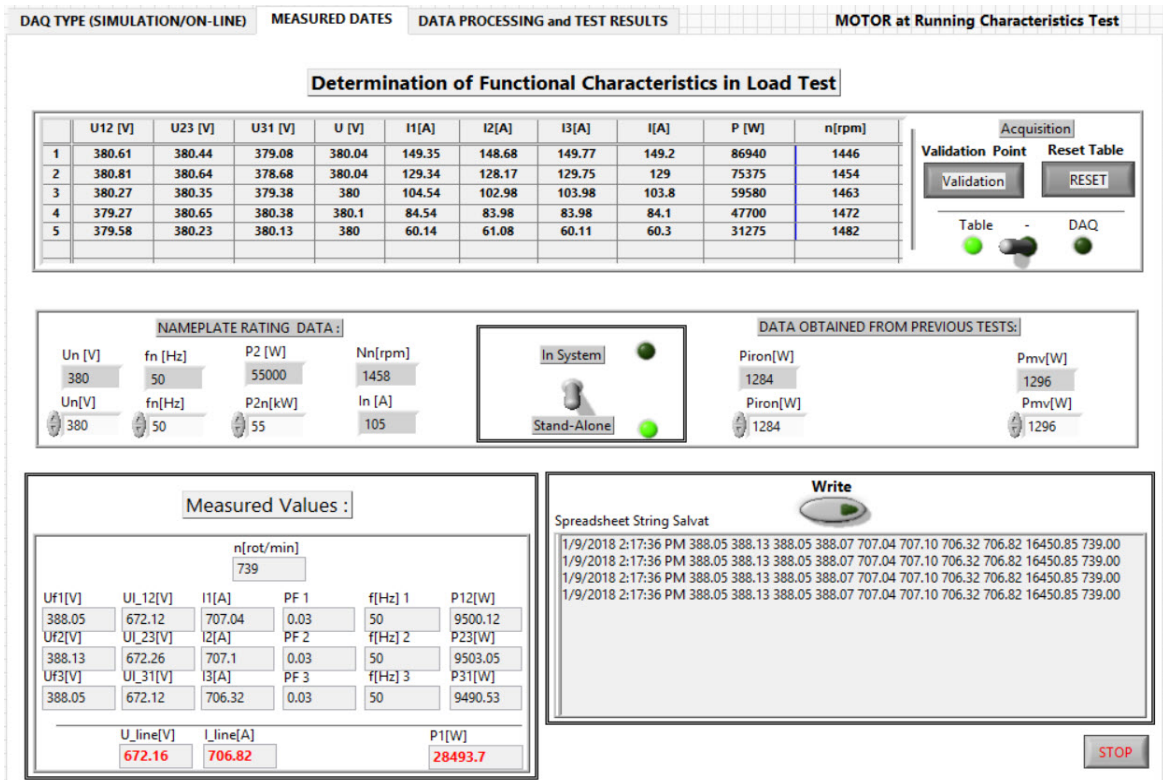


Fig. 11. The front panel of *Running-Characteristics Test.vi* (Page 2: Measured Dates)

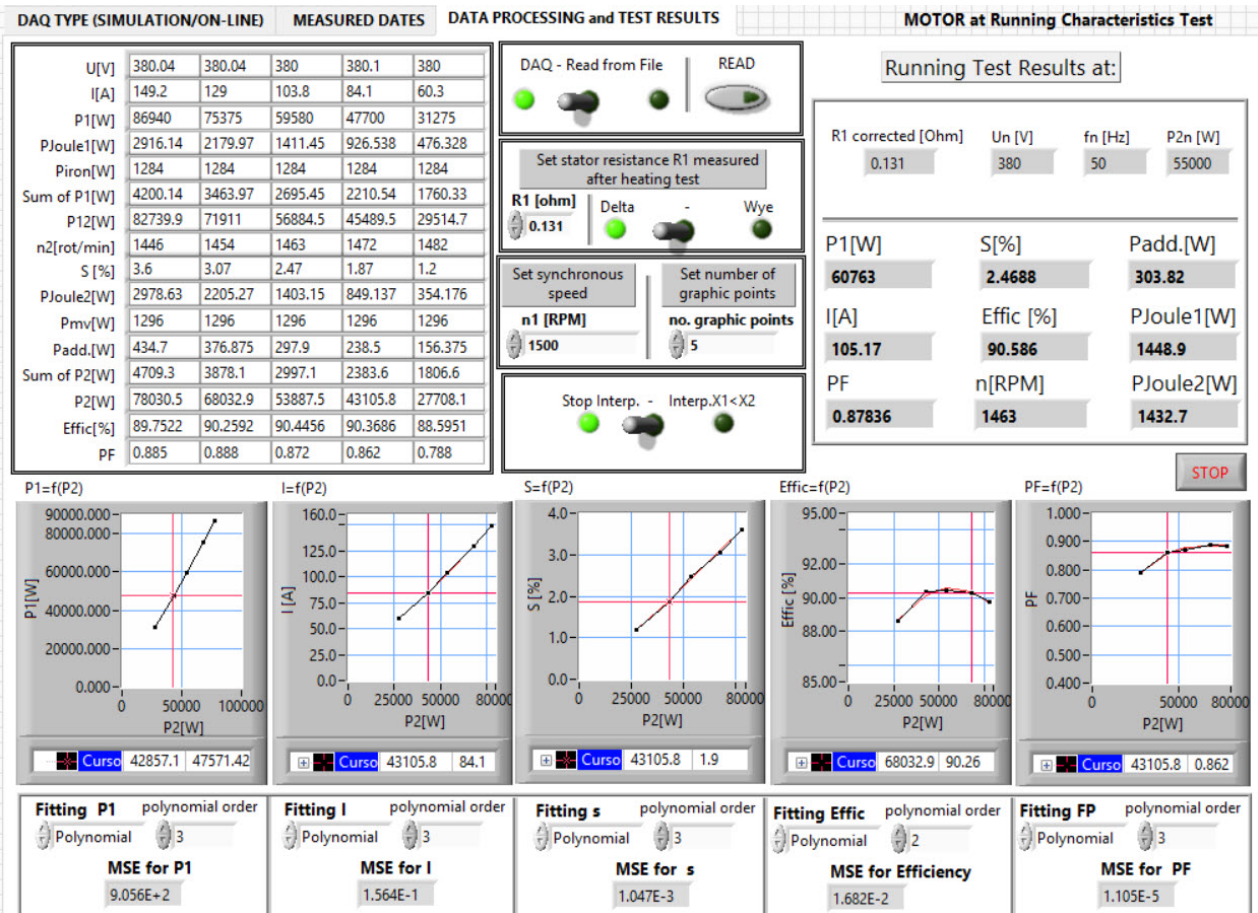


Fig. 12. The front panel of *Running-Characteristics Test.vi*. (Page 3: Data Processing and Test Results)

## V. RESULTS AND THEIR INTERPRETATION

The advanced testing system proposed in this document was checked in the testing laboratory of electrical rotating machines at the University of Craiova, Faculty of Electrical Engineering.

An three-phase induction motor with the following nameplate rating data: type MIB3 250M 65-4; connection  $\Delta$ ;  $P = 55 \text{ kW}$ ;  $U = 380 \text{ V}$ ;  $I = 105 \text{ A}$ ;  $n = 1458 \text{ r/min}$ ;  $PF = 0.89$ ;  $f = 50 \text{ Hz}$ ; Efficiency ( $\eta$ ) = 92%;  $Mp/Mn = 2.6$ ;  $I_p/I_n = 6.5$ ; Protection of Motor: IP44; Insulation Class F has been tested.

Next I will refer to the results obtained in the case of two tests, namely: no-load test and running characteristics test. I had available the documentation from the motor approval with the data of the type test.

The no-load test report data are presented in Table 1 (11 points of measurement; the absorbed power was measured by the two wattmeter method; the phase stator winding resistance  $R_l$  which was determined after test had the value  $0.1034 \Omega$ ).

In Fig. 10 it is observed that for the nominal value of the supply voltage  $U_0 = 380 \text{ V}$  the following no-load values are obtained:

- no-load power  $P_0 = 2717.6 \text{ W}$ ;
- no-load current  $I_0 = 36.486 \text{ A}$ ;
- power factor  $PF_0 = 0.11$ ;
- mechanical and ventilation losses  $P_{mv} = 1295.9 \text{ W}$ ;
- iron losses  $P_{iron} = 1283.99 \text{ W}$ ;
- Joule stator losses  $P_{Joule0} = 137.65 \text{ W}$ .

Figure 13 shows the millimeter paper plot of the  $I_0 = f(U_0)$ ,  $P_0 = f(U_0)$  and  $P_0 = f(U_0^2)$  graphs and the classical determination of the test parameter values:

- no-load power  $P_0 = 2712 \text{ W}$ ;
- no-load current  $I_0 = 36.6 \text{ A}$ ;
- power factor  $PF_0 = 0.11$ ;
- mechanical and ventilation motor losses  $P_{mv} = 1320 \text{ W}$ ; iron losses  $P_{iron} = 1254 \text{ W}$  and Joule losses  $P_{Joule0} = 138 \text{ W}$ .

TABLE I.  
THE INPUT DATA FOR CONVENTIONAL NO-LOAD TESTING

U	I <sub>1</sub>	I <sub>2</sub>	I <sub>3</sub>	I <sub>0</sub>	+W <sub>2</sub>	-W <sub>1</sub>	ΣW	P <sub>0</sub>
[V]	[A]	[A]	[A]	[A]	[W]	[W]	[W]	[W]
389	97.5	99.7	97.7	39.3	73.7	49.9	23.8	2856
<b>380</b>	<b>91.3</b>	<b>92.7</b>	<b>90.7</b>	<b>36.6</b>	<b>67.4</b>	<b>44.8</b>	<b>22.6</b>	<b>2712</b>
362	78.5	79.9	78.3	31.6	56.4	35.8	20.6	2472
330	63.1	64.1	63.0	25.4	43.1	24.3	18.8	2256
301	53.5	54.1	53.3	21.4	34.9	17.2	17.7	2124
267	90.5	91.5	90.0	18.1	54.8	22.8	32.0	1920
242	80.5	81.2	80.2	16.1	45.8	16.0	29.8	1788
211	69.7	70.1	69.3	13.9	110.1	26.8	88.3	1766
191	64.2	65.0	63.9	12.9	98.8	12.0	86.8	1736
171	59.2	59.8	58.8	11.8	84.9	-4.1	80.8	1616
151	54.8	55.5	54.8	10.8	73.4	+4.1	77.5	1550

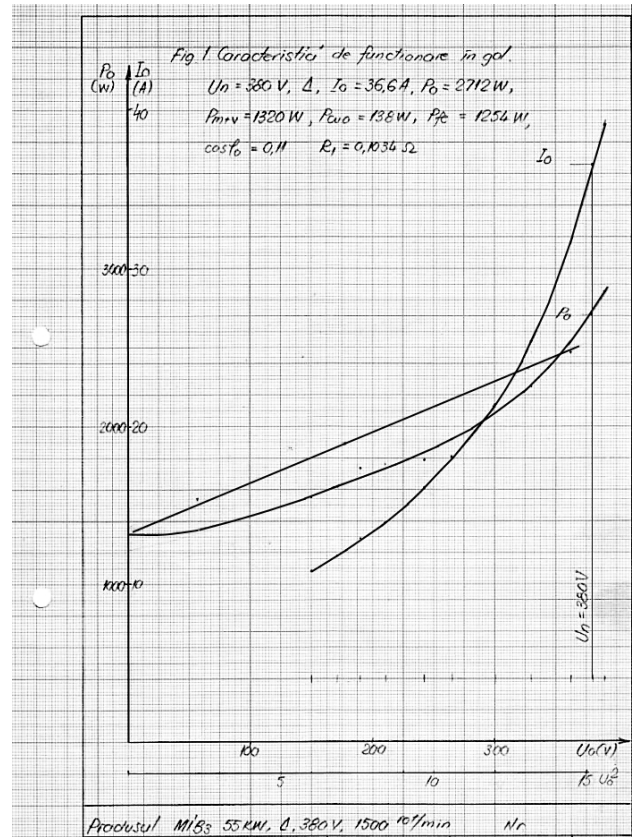


Fig. 13. Photocopy of the result of classical no-load test.

The values of the parameters obtained with the proposed system (see Fig. 10) are comparable to those obtained by conventional methods (see Fig. 13).

The value of a DC resistance ( $R_l$ ) at ambient temperature ( $T_{amb} = 28.3^\circ\text{C}$ ) determined with VI is  $0.098\Omega$  compared to  $0.0992\Omega$  from the test report; the value corrected at the temperature ( $T_l = 115^\circ\text{C}$ ) determined with VI is  $0.13199\Omega$  compared to  $0.131\Omega$  from the report.

The input data for conventional running test are displayed in Table II; they are values acquired for voltage, current, power absorbed and motor speed in 5 measuring points.

Figure 14 shows the millimeter paper plot of the curves  $P_1 = f(P_2)$ ,  $I_1 = f(P_2)$ ,  $s = f(P_2)$ ,  $\eta = f(P_2)$ ,  $PF = \cos\varphi = f(P_2)$  and the classical determination of functional characteristics in load test.

TABLE II.  
THE INPUT DATA FOR CONVENTIONAL RUNNING TESTING

U	[V]	380	380	380	380	380
I <sub>1</sub>	[A]	150	128.25	103.95	84.3	60.75
I <sub>2</sub>	[A]	149.7	130.2	104.25	84	60
I <sub>3</sub>	[A]	148.2	128.4	103.2	84	60.3
I	[A]	149.2	129	103.8	84.1	60.3
W <sub>1</sub>	[W]	56115	48825	38790	31950	22500
W <sub>2</sub>	[W]	30825	26550	20790	15750	8775
P <sub>1</sub>	[W]	86940	75375	59580	47700	31275
n <sub>2</sub>	[rpm]	1446	1454	1463	1472	1482

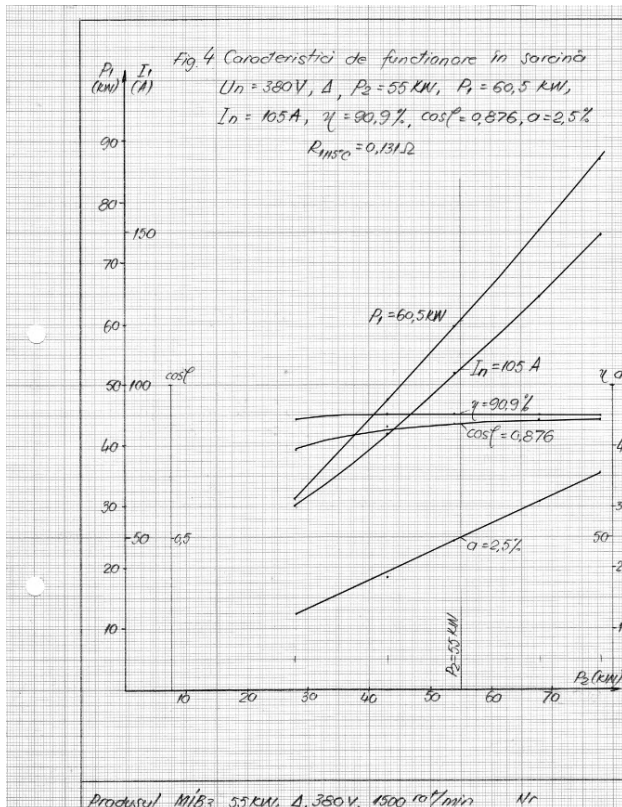


Fig. 14. Photocopy of the result of classical running in load test.

The values obtained by classical determination for these parameters (at rated voltage  $U_N = 380\text{V}$  and rated output power  $P_{2N} = 55\text{kW}$ ) are:

- input power  $P_1 = 60.5\text{ kW}$ ;
- input current  $I_1 = 105\text{ A}$ ;
- efficiency  $\eta = 90.9\%$ ;
- power factor  $PF = 0.876$ ;
- slip  $s = 2.5\%$ .

The values of these parameters obtained with the proposed system (see Fig. 12) are presented below:

- input power  $P_1 = 60.76\text{ kW}$ ;
- input current  $I_1 = 105.17\text{ A}$ ;
- efficiency  $\eta = 90.58\%$ ;
- power factor  $PF = 0.878$ ;
- slip  $s = 2.46\%$ .

The values of the motor parameters obtained by the two methods (classical, by drawing on the millimeter paper and the proposed advanced system) are comparable with a good accuracy.

## VI. CONCLUSIONS

A comparison between the advanced virtual measurements system and classical results shows that the proposed solution is correct, reliable and compatible.

The results obtained recommend the virtual measurement system in industry applications: it is a very competitive, complete, complex and flexible system, ready to move the testing bench in industry to the next generation of equipment, technology and methodology.

With his interactive simulation function, the virtual measurement system would be very useful to a help for

the University and college students in the process of learning the theory about electrical machines.

The system can be easy updated and customized in the future with another data acquisition module and virtual instruments.

## ACKNOWLEDGMENT

**Source of research funding in this article:** Research program of the Electrical Engineering Department financed by the University of Craiova.

Received on July 17, 2018

Editorial Approval on November 15, 2018

## REFERENCES

- [1] T. Wildi, *Three-phase induction machines*, in *Electrical machines, drives, and power systems*, 6th ed., Upper Saddle River, New Jersey, USA: Pearson Prentice Hall, 2006, pp. 263-284.
- [2] A.E. Fitzgerald, C. Kingsley Jr., and S.D. Umans, *Polyphase induction machines*, in *Electric machines*, 6th ed., Ed. New York, NY, USA: McGraw-Hill, 2003, pp. 306-356.
- [3] Ghe. E. Subtirelu, "Advanced system for testing of three-phase induction machines," *Proceedings of 2018 International Conference on Applied and Theoretical Electricity ICATE*, October 4-6, 2018, Craiova, Romania, IEEE Catalog No. CFP1899S-USB, ISBN: 978-1-5386-3805-7.
- [4] E. Subtirelu, M. Dobriceanu, "Virtual measurement system for study and determination parameters in asynchronous motor test", *IEEE Xplore*, pp. 469-474, 2008 IEEE International Symposium on Power Electronics, Electrical Drives, Automation and Motion (SPEEDAM), 11-13 June 2008, Ischia, Italy, ISBN 978-1-4244-1664-6, DOI: 10.1109/SPEEDHAM.2008.4581312.
- [5] G.E. Subtirelu, M. Dobriceanu, "Virtual instruments (VIs) for study of asynchronous motor functional characteristics," *IEEE Xplore*, pp. 1-6, 2011 IEEE International Symposium on Advanced Topics in Electrical Engineering (ATEE), 12-14 May 2011, Bucharest, Romania, ISBN: 978-1-4577-0507-6.
- [6] G.E. Subtirelu, M. Dobriceanu, M.A. Enache, N. Boteanu, "Virtual instrument for study dynamic regimes of variable reluctance synchronous motors," *IEEE Xplore*, pp. 1-6, 2014 IEEE International Conference on Applied and Theoretical Electricity (ICATE), 23-25 Oct. 2014, Craiova, Romania, ISBN: 978-1-4799-4161-2, DOI: 10.1109/ICATE.2014.6972640Y.
- [7] H. Calis, E. Caki, "LabVIEW based laboratory typed test setup for the determination of induction motor performance characteristics", *Journal of Electrical Engineering and Technology*, November, 2014, vol. 9, no. 6, pp. 1928-1934, DOI: 10.5370/JEET.2014.9.6.1928.
- [8] S. Renyin, "Research on testing system of asynchronous motor based on LabVIEW", *Book Series: AER-Advances in Engineering Research*, Volume: 107 Pages: 401-404, Published: 2017, Proceedings of the 2016 2nd International Conference on Materials Engineering and Information Technology Applications (MEITA 2016), WOS:000429966800083, ISBN:978-94-6252-304-3, ISSN: 2352-5401.
- [9] H.E. Jordan, R.C. Zowarka, T.J. Hotz, J.R. Uglum, "Induction motor performance testing with an inverter power supply", *IEEE Transactions on Magnetics*, vol. 43, no. 1, January 2007, pp. 242-245.
- [10] E.J. Wiedenbrug, A. Ramme, E. Matheson, A. von Jouanne, A.K. Wallace, "Modern online testing of induction motors for predictive maintenance and monitoring", *IEEE Transactions on Industry Applications*, Volume: 38, Issue: 5, Sep/Oct 2002, Page(s): 1466 - 1472, INSPEC Accession Number: 7407561, DOI: 10.1109/TIA.2002.802992.
- [11] LabVIEW Fundamentals, *National Instruments*, p.n. 374029A - 01, 2005.
- [12] IEEE Test procedure for polyphase induction motors and generators, *IEEE Standard 112*, 2004.



- [13] IEC Rotating electrical machines - Part 1: Rating and performance, *IEC Standard 60034-1*, 2017.
- [14] IEC Rotating electrical machines - Part 2-1: Standard methods for determining losses and efficiency from tests (excluding machines for traction vehicles), *IEC Standard 60034-2-1*, 2014.
- [15] ASRO Three phase asynchronous motors. Test methods, *ASRO Standard SR7246*, 1998 (In Romanian).